Int. J. Electrochem. Sci., 11 **(2016)** 1472 - 1481

International Journal of
ELECTROCHEMICAL
SCIENCE
www.electrochemsci.org

Short Communication

Characterization and Application of Electrospun Prussian Blue Nanofibers Synthesized by Electrospinning Polyacrylonitrile Solution

Kyung-Hee Park[1], *Do-Young Choi*[2], *Joon-Hyung Park*[3], *Chan Kim*[4], *Tae-Young Kim*[5], *Jae-Wook Lee*[3,*]

[1]Department of Dental Materials and Medical Research Center for Biomineralization Disorders, School of Dentistry, Chonnam National University, Gwangju 500-757, Korea
[2]KHT Engineering Co., Gunpo 435-73, Korea
[3]Department of Chemical and Biochemical Engineering, Chosun University, Gwangju 501-759, Republic of Korea
[4]Amotech New Materials Research Center, Gimpo 597-2, Republic of Korea
[5]Department of Environmental Engineering, Chonnam National University, Gwangju 500-757, Republic of Korea
[*]E-mail: jwlee@chosun.ac.kr

Received: 11 September 2015 / *Accepted:* 19 November 2015 / *Published:* 1 January 2016

Electrospinning technique is a powerful and effective method for the preparation of nanofibers. Here we demonstrated an efficient prussian blue (PB) nanofibers prepared by the electrospinning method using polyarylonitrile as a precursor. The samples were characterized by scanning electron microscopy, thermogravimetric analysis, energy-dispersive X-ray spectroscopy and Brunauer-Emmet-Teller method. The adsorption equilibrium data were obtained at different temperatures and fitted with the Langmuir isotherm. We found that the novel PB nanofibers could efficiently remove the cesium ions dissolved in water.

Keywords: Electrospinning, Prussian blue, Polyacrylonitrile, Cesium adsorption

1. INTRODUCTION

Since their accidental release at Chernobyl (1987) and the Fukushima Daiichi nuclear power plant (2011), radionuclides are a major concern to human health. Radioactive cesium is of particular concern because of its high radioactivity and long half-life (30.2 ys), which is much longer than that of iodine (8d) [1,2]. It has been known that adsorption is a simple and economic technique for the removal of radioactive cesium. The main advantage of adsorption is not required the further treatment processes after removal of the targeted element from the adsorbents. Several adsorbents including

zeolite, activated carbon, polymers, and biomass have already been reported [3,4]. However, a limitation of these adsorbents is a selective cesium removal for the adsorption sites with alkali and alkaline earth metals, such as potassium, sodium, calcium, and magnesium compete with cesium [5]. Therefore, novel adsorbents with highly specific to cesium, rather than to other alkali and alkaline earth metals, are needed.

Prussian blue (PB) has been employed for the removal of radioactive cesium from the gastrointestinal tracts of animals by oral administration [6-8]. PB, as an excellent adsorbent of cesium, is a dark blue pigment with the chemical formula $Fe_4[Fe(CN)_6]_3 \cdot XH_2O$ (X=14-16) and a cubic face centered lattice structure [9,10]. Recently, PB nanoparticles and PB caged in matrices of nonwoven fabric, spongiform, alginate/calcium beads, and cotton gauze have been utilized for the removal of radioactive cesium. However, an efficient adsorbent with higher adsorption capacity and faster kinetics should be developed. In a sense, PB nanofiber seems to be an excellent candidate for the removal of cesium ions from aqueous solutions. Electrospun fibers have attracted great interest for a wide range of applications such as tissue engineering, sensors, protective clothing, high-performance filters, and functional nanomaterials [11]. Electrospinning has been proven to be a powerful and effective method for the preparation of nanofibers. This process produces nanofibers by applying a high voltage to a polymer solution or a melt, using the repulsive electro-static force by the electric field applied between the two electrodes [12,13].

In this work, we demonstrate the potential of the polyacrylonitrile (PAN)-based PB nanofibers as a novel adsorbent for the removal of cesium dissolved in water. To this end, the elctrosupn PB nanofibers were prepared and characterized by scanning electron microscopy, thermogravimetric analysis, energy-dispersive X-ray spectroscopy and Brunauer-Emmet-Teller method. For the systematic analysis of PB nanofibers, the adsorption equilibrium data at different temperatures were obtained and the thermodynamic properties were determined by applying the Van't Hoff equation.

2. EXPERIMENT

2.1. Preparation of adsorbents

A 15 wt.% PAN solution was prepared in *N*,*N*-dimethylformamide (DMF). The solution was mixed with PB particle of 1-20wt% of PB particles using a paste mixer. The mixed solution was spun into a fiber by passing it through a positively charged capillary, using an electrospinning apparatus set at a dc voltage of 20 kV (NT-PS-35K, NTSEE Co., Korea). The negative electrode was connected to a drum winder wrapped with aluminum foil, which served as the fiber collector. For comparison with PAN, polyvinylidene fluoride (PVDF, M.W. = 534,000, Sigma–Aldrich) was used as a precursor.

2.2. Characterization of adsorbents

The PB fiber surface was analyzed using a scanning electron microscope (SEM, Hitachi, S-4700, Japan). The C, N, O, Na, K and Fe contents in the PB fiber samples were determined using an elemental analyzer (EA) (Fisions EA 1110 CHNS-O, Thermo Quest). The thermal behavior of the PB

fibers was evaluated by thermogravimetric analysis (TGA) (STAR SW, Mettler) conducted up to 1,000 °C, at a heating rate of 5 °C/min under a nitrogen atmosphere. To determine the surface area of the prepared PB nanofibers, the nitrogen adsorption and desorption were measured after preheating the samples to 150 °C for 2 h to eliminate surface contaminants and adsorbed water, using a nitrogen adsorption analyzer (ASAP 2020, Micromeritics). The pore volume and pore size distributions were obtained by applying the Horvath-Kawazoe (HK) and the Barrett-Joyner-Halenda (BJH) equations.

2.3. Batch adsorption experiments

The adsorption equilibrium data were measured by introducing a given amount of PB fibers into an aqueous solution of cesium, with an appropriate concentration (100 mg/L), followed by continuously shaking the adsorbates in a constant-temperature incubator, set at 10, 30, and 50 °C for 46 h to allow sufficient contact time for equilibrium. After shaking, the samples were removed from the flasks and filtered through a 0.2 μm filter paper (ADVANTEC, Japan). The filtrate was then analyzed to measure the cesium concentration. The cesium adsorption capacity of the PB fibers was calculated using

$$q = \frac{(C_0 - C)}{w} V \quad (1)$$

where q (mg/g) is the adsorbed amount, w (g) is the weight of the adsorbent, C_0 and C (mg/L) are the initial and equilibrium concentration of cesium in solution, respectively, and V (L) is the volume. The cesium concentrations were analyzed using an inductively coupled plasma mass spectrometer (ICP-MS, NexIon 300D, Perkin-Elmer Co., Ltd.)

3. RESULTS AND DISCUSSION

3.1. Characterization

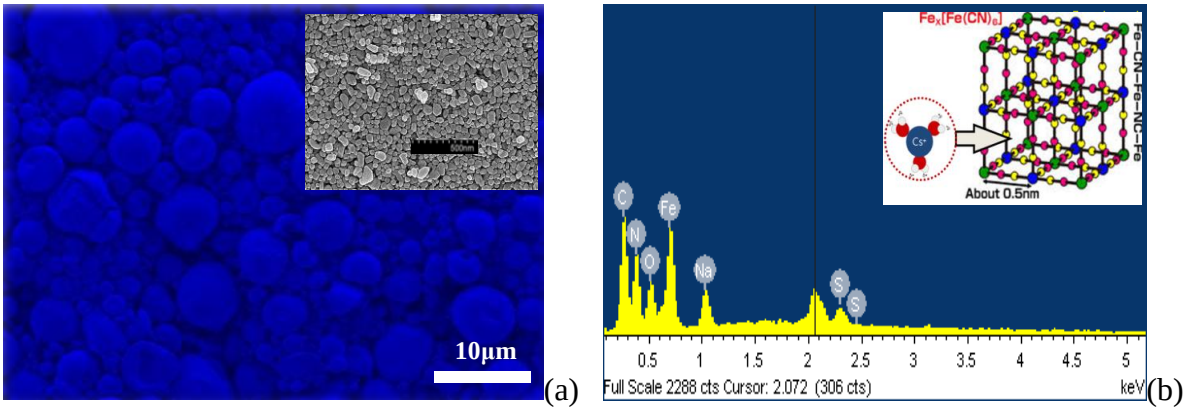

Figure 1. The FE-SEM images (a) and EDX spectrum (b) of the PB particles.

Figure 1 shows the FE-SEM images and EDX spectrum of the PB particles. Elemental analysis of the PB particles revealed the presence of C, O, N, Fe, Na, S, and Fe. As expected from the chemical

formula, the elemental contents of Fe, C and N were higher (Table 1). From the TGA/DTG analysis, we found that the sudden and sharp increase in weight loss of the PB particles began at 220 °C and the final yields at 570 °C under nitrogen was 40% (Figure 2).

Table 1. EDX spectra of the PB particles

Element	Weight %	Atomic %
C	21.4	34.0
N	26.2	35.8
O	12.2	14.6
Na	3.2	2.66
S	1.1	0.7
Fe	35.9	12.3

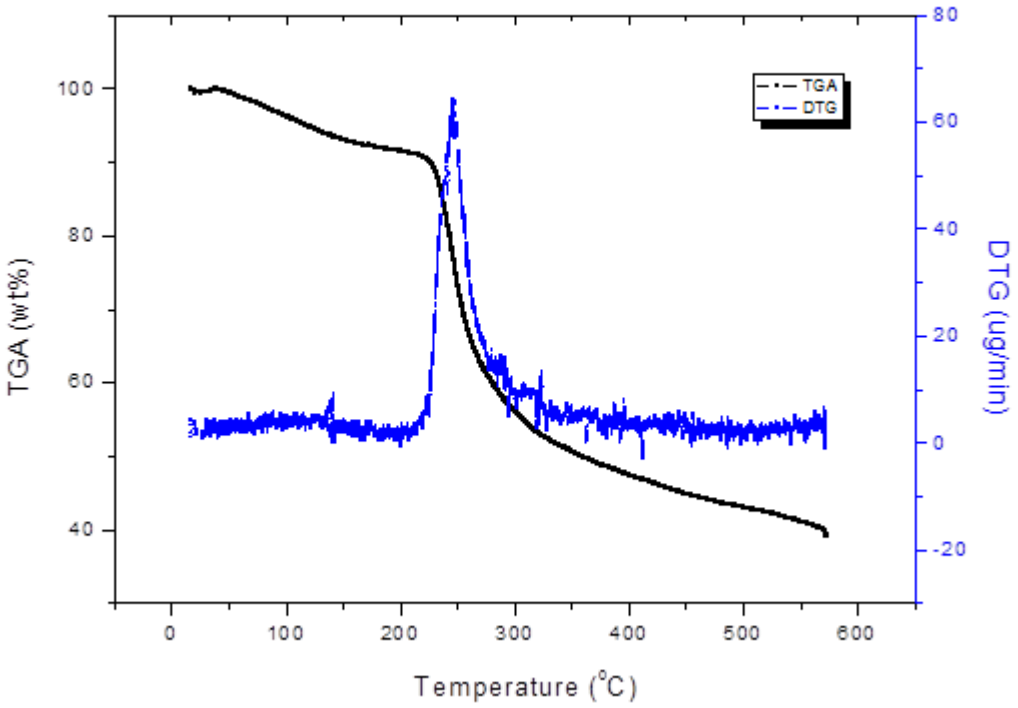

Figure 2. TGA curves for the PB particles under nitrogen atmospher.

The SEM images of the electrospun PAN and PB-PAN fibers according to their different (from 1 to 20%) PB content are shown in Figure 3. The electrospun PVP and PB/PVP fibers were uniform in size and had smooth morphologies. The diameters of the electrospun fibers increased slightly upon increasing the PB content (Figure 4). The average diameter of the electrospun fibers was evaluated by selecting 100 fibers from the ×1000 magnification SEM images and analyzing them using a custom code image-analysis program. The average diameters of the fibers were in the range of 200-1200 nm. In addition, the surface area and average pore size of the PB fibers were 40 m^2/g and 66.5 nm,

respectively and were determined, using adsorption isotherm data by the BET and BJH methods, respectively (not shown here).

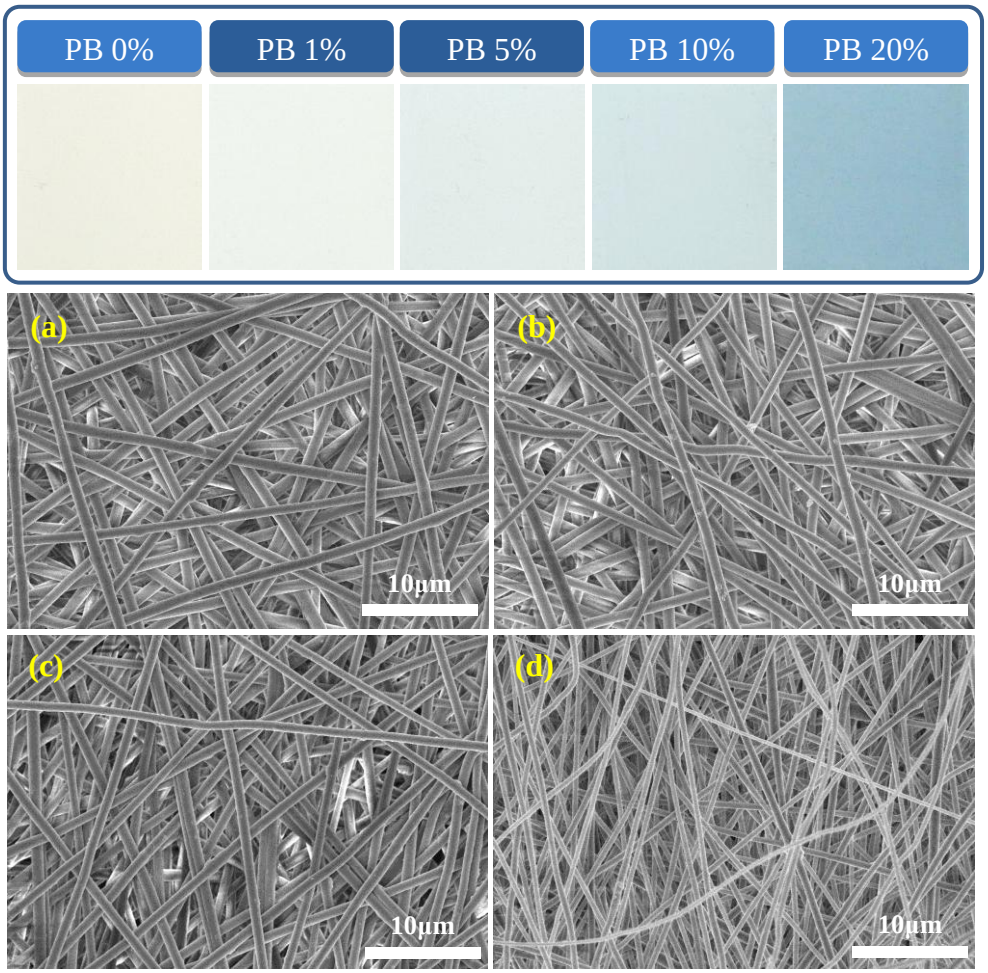

Figure 3. The optical and SEM images of PAN (a), 5%-PB/PAN (b), 10%-PB/PAN (c), and 20%-PB/PAN (d).

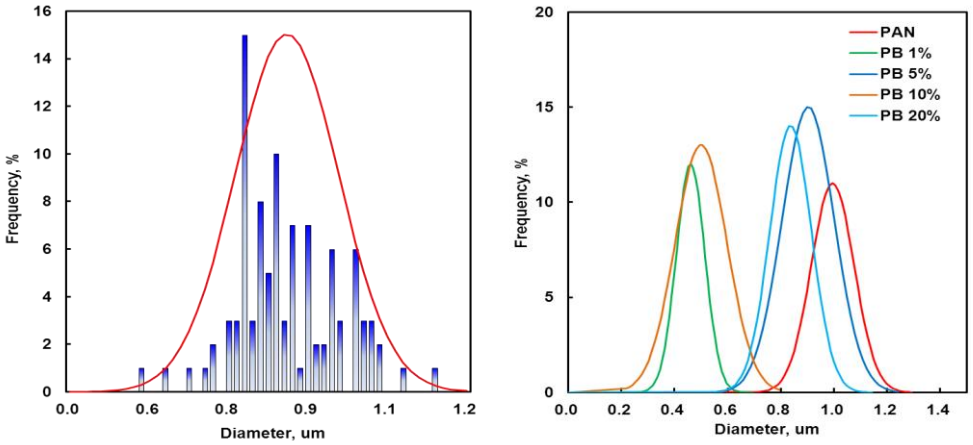

Figure 4. The fiber-diameter distribution of PAN (left) and PB/PAN at different particle loadings (right).

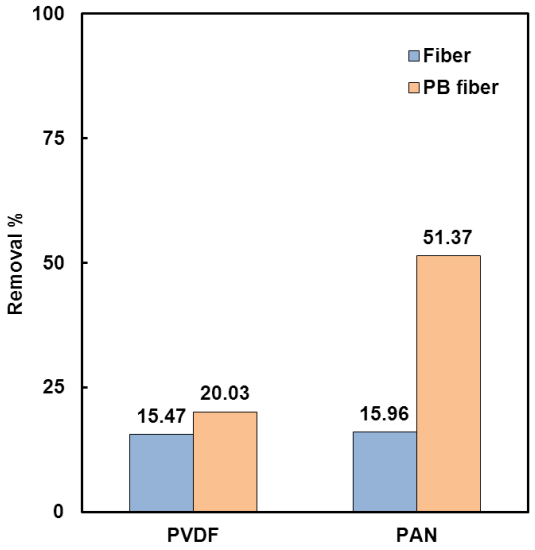

Figure 5. Adsorption removal efficiency of PVDF- and PAN-based fibers.

Figure 5 shows the efficiency of the PVDF-based and PAN-based PB fibers for the removal by adsorption of cesium dissolved in water. As expected, the adsorption capacity of the hydrophilic PAN-based PB fiber was greater than that of the hydrophobic PVDF-based fiber. The removal efficiency of the PB/PAN fiber was 51.37%.

3.2. Adsorption behavior

The adsorption isotherm data of cesium were measured at three different temperatures (10, 30, and 50 °C). The results show that the adsorption amount increased with increasing temperature. This result implies that the contribution of chemisorption requires activation energy to be overcome and therefore, is more efficient at higher temperatures (Figure 5). The equilibrium data of the adsorption of cesium on PB fibers well correlated with the Langmuir equation:

$$q = q_m bC/(1+bC) \quad (2)$$

The isotherm parameters were determined, based on a modified Levenberg-Marquardt method (IMSL routine DUNSLF), by minimizing the mean percentage deviations between the experimental and predicted adsorbed capacity. The object function (*E(%)),* which represents the average percent deviation between the experimental and predicted results is as follows:

$$E(\%) = 100/n\sum_{k=1}^{n}[|q_{\exp,k} - q_{cal,k}|/q_{\exp,k}] \quad (3)$$

Here, n is the number of experimental data, $q_{exp,k}$ is the experimental adsorption data, and $q_{cal,k}$ is the calculated adsorption data. The solid lines in Figure 6 are the predicted results, based on the Langmuir isotherm parameters (Table 2)

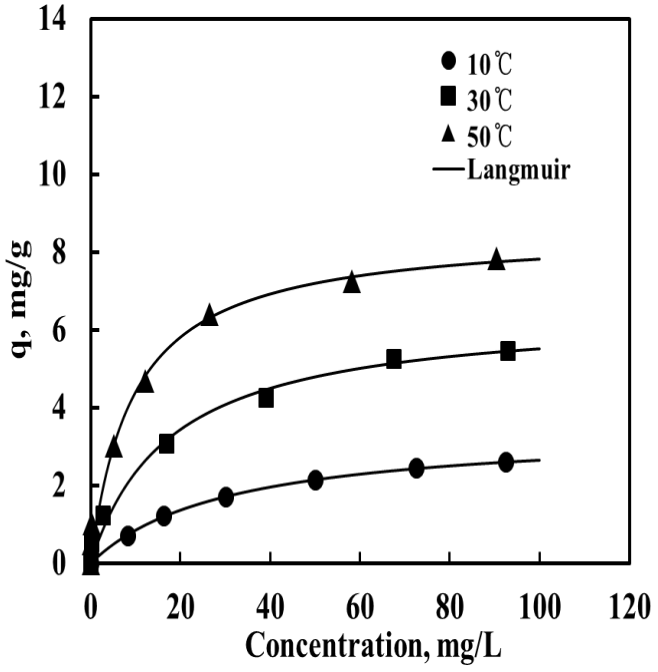

Figure 6. Adsorption isotherms of cesium on electrospun PB/PAN fibers at different temperatures (10, 30, and 50 ^{o}C).

Table 2. Langmuir isotherm parameters of cesium on 20%-PB/PAN at different temperatures

Temperature (℃)	Parameters		
	q_m	*b*	*E(%)*
10	3.47	0.03	0.001
30	6.49	0.06	0.423
50	8.56	0.11	0.724

It has been recognized that surface heterogeneity may result from either energetic, structural, or geometric heterogeneity [14,15]. As a measure of the energetic heterogeneity of a solid surface, the isosteric enthalpy has been employed to determine the degree of interaction between the adsorbate molecules and adsorbent lattice atoms. In general, the isosteric enthalpy curve varies with the surface loading for a heterogeneous adsorption system. The isosteric enthalpies of cesium adsorption were calculated using the Clausius-Clapeyron equation [16]:

$$q_{st} = -R\left[\partial \ln C / \partial (1/T)\right]_q \quad \textbf{(4)}$$

where q_{st} is the isosteric enthalpy, R is the gas constant, C is the concentration, and T is the temperature. The results show that the isosteric enthalpy of cesium adsorption increased in the range of 40 - 140 kJ/mol (Figure 7).

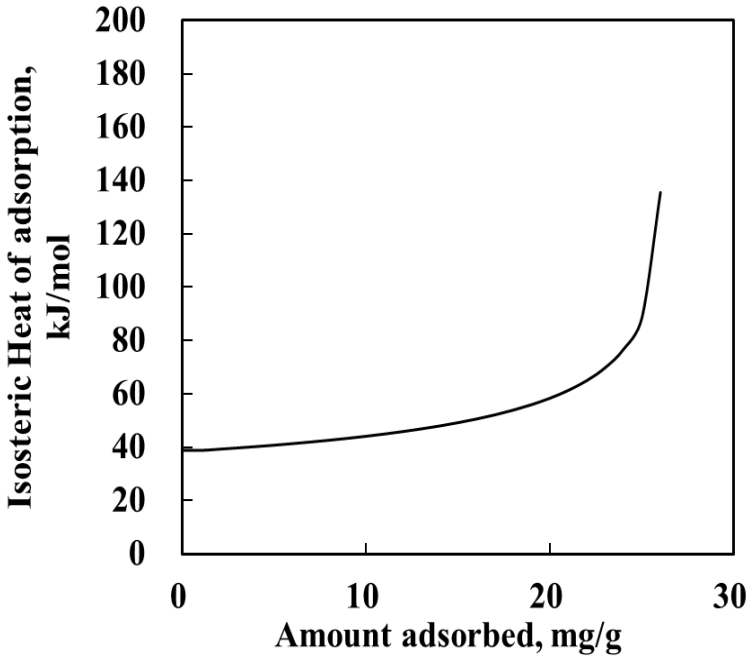

Figure 7. The isosteric heat of adsorption of cesium on electrospun PB/PAN fibers.

At a particular temperature, the equilibrium constant (*b*) is related to the change in Gibbs free energy (Δ*G*), entropy change (Δ*S*), and the heat of adsorption (Δ*H*) at a constant temperature by the the Van't Hoff equation:

$$\Delta G = \Delta H - T\Delta S \quad (5)$$

$$\ln(q_m b) = \frac{\Delta S}{R} - \frac{\Delta H}{RT} \quad (6)$$

where R= 8.314 J/mol/K is the gas constant and T is the temperature in Kelvin. The enthalpy of adsorption (Δ*H*) and the entropy change (Δ*S*) were determined from the slope and intercept of the linear plot of ln($q_m b$) vs. 1/*T*. The calculated thermodynamic values of Δ*G*, Δ*H*, and Δ*S* are listed in Table 3. The negative values of Δ*G* indicate that the adsorption of cesium onto PB fibers is a spontaneous process. On the other hand, the positive value of the standard enthalpy change (Δ*H*) implies that the adsorption of cesium by electrospun PB fibers is endothermic. In this case, the adsorption of cesium increased at higher temperatures.

Table 3. The thermodynamic properties for cesium adsorption on 20%-PB/PAN at different temperatures

ΔG° (kJ/mol)			ΔH° (kJ/mol)	ΔS° (kJ/mol)
10℃	30℃	50℃		
-9.49	-10.17	-10.84	22.36	33.63

4. CONCLUSIONS

We have successfully prepared PB nanofibers by the electrospinning method using PVA as a precursor. The average diameters of the fibers were in the range of 200-1200 nm. The surface area and average pore size of the PB fibers were 40 m^2/g and 66.5 nm, respectively. The adsorption equilibrium revealed that the adsorption capacity of cesium on PB nanofibers increased with increasing temperature (i.e., endothermic adsorption). The adsorption isotherm data showed good correlation with the Langmuir isotherm and the maximum adsorption capacity was 8 mg/g. It was found that the novel PB nanofibers prepared in this work could efficiently remove radioactive cesium dissolved in water.

ACKNOWLEDGEMENTS
This work was supported by the Human Resources Development program (No. 20134010200560) of the Korea Institute of Energy Technology Evaluation and Planning (KETEP) grant funded by the Korea government Ministry of Trade, Industry, and Energy.

References

1. X. Liu, G.R. Chen, D.J. Lee, T. Kawamoto, H. Tanaka, M.L. Chen, Y.K. Luo, *Bioresource Technol.* 160 (2014) 142.
2. A. K. Vipin, B. Hu, B. Fugetsu, *J. Hazard. Mater.* 258 (2013) 93.
3. C. Thammawong, P. Opaprakasit, P. Tangborilboonrat, P. Sreearunothai, *J. Nanopart. Res.* 15 (2013) 1689.
4. B. Hu, B. Fugetsu, H. Yu, Y. Abe, *J. Hazard. Mater.* 217 (2012) 85.
5. T. Sangvanich, V. Sukwarotwat, R.J. Wiacek, R.M. Grudzien, G.E. Fryxell, R.S. Addleman, C. Timchalk, W. Yantasee, *J. Hazard. Mater.* 182 (2010) 225.
6. M.R. Awual, S. Suzuki, T. Taguchi, H. Shiwaku, Y. Okamoto, T. Yaita, *Chem. Eng. J.* 242 (2014) 127.
7. A. Kitajima, H. Tanaka, N. Minami, K. Yoshino, T. Kawamoto, *Chem. Lett.* 41 (2012) 1473.
8. M. Ishizaki, S. Akiba, A. Ohtani, Y. Hoshi, K. Ono, M. Matsuba, T. Togashi, K. Kananizuka, M. Sakamoto, A. Takahashi, T. Kawamoto, H. Tanaka, M. Watanabe, M. Arisaka, T. Nankawa, M. Kurihara, *Dalton Trans.* 42 (2013) 16049.
9. A. Kitajima, H. Ogawa, T. Kobayashi, T. Kawasaki, Y. Kawatsu, T. Kawamoto, H. Tanaka, *Envioron. Sci.: Processes Impacts* 16 (2014) 28.

10. S. Tsuruoka, B. Fugetsu, F. Khoerunnisa, D. Minami, K. Takeuchi, M. Fujishige, T. Hayashi, Y. A. Kim, K.C. Park, M. Asai, K. Kaneko, M. Endo, *Mater. Express* 3 (2013) 21.
11. J.H. Kim, K.H. Park, T.Y. Kim, S.J. Yoo, D.H. Kwak, H.J. Jung, J.W. Lee, *Nanoscale Res. Lett.* 9 (2014) 44.
12. C. Kim, Y.I. Jeong, B.T.N. Ngoc, K.S. Yang, M. Kojima, Y.A. Kim, M. Endo, J.W. Lee, *Small* 3(1) (2007) 91.
13. M.A. Abu-Saied, K.A. Khalil and S.S. Al-Deyab, *Int. J. Electrochem. Sci.* 7 (2012) 2019.
14. K.J. Hwang, S.H. Jung, D.W. Park, S.J. Yoo, J.W. Lee, W.G. Shim, *Curr. Appl. Phys.* 10 (2010) S184.
15. K.J. Hwang, W.G. Shim, S.H. Jung, S.J. Yoo, J.W. Lee, W.G. Shim, *Appl. Surf. Sci.* 256 (2010) 5428.
16. Y. Jiang, Y. Yuan, K. Wang, H. Li, C. Xu, X. Yang, *Int. J. Electrochem. Sci.* 7 (2012) 10933.

© 2016 The Authors. Published by ESG (www.electrochemsci.org). This article is an open access article distributed under the terms and conditions of the Creative Commons Attribution license (http://creativecommons.org/licenses/by/4.0/).